

Chondrosarcoma with Target-Like Chondrocytes: Update on Molecular Profiling and Specific Morphological Features

(cartilage tumour / chondrocytes with thick pericellular rings / target-like chondrocyte / immunohistochemistry / electron microscopy / *FNI-FGFR2* gene fusion)

C. POVÝŠIL¹, J. HOJNÝ¹, M. KAŇA²

¹Institute of Pathology, First Faculty of Medicine, Charles University and General University Hospital in Prague, and Institute of Postgraduate Studies, Prague, Czech Republic

²Department of Otorhinolaryngology, Head and Neck Surgery, First Faculty of Medicine, Charles University and University Hospital Motol, Prague, Czech Republic

Abstract. This is the first histological and molecular analysis of two chondrosarcomas with target-like chondrocytes that were compared with a group of conventional chondrosarcomas and enchondromas. The unique histological feature of target-like chondrocytes is the presence of unusual hypertrophic eosinophilic APAS-positive perichondrocytic rings (baskets). In the sections stained with Safranin O/Fast green, the outer part of the ring was blue and the material in the lacunar space stained orange, similarly to intercellular regions. Immunohistochemical examination showed strong positivity for vimentin, factor XIIIa, cyclin D1, osteonectin, B-cell lymphoma 2 apoptosis regulator (Bcl-2), p53 and p16. The S-100 protein was positive in 25 % of neoplastic cells. Antibodies against GFAP, D2-40 (podoplanin), CD99, CKAE1.3 and CD10 exhibited weak focal positivity.

Pericellular rings/baskets contained type VI collagen in their peripheral part, in contrast to the type II collagen in intercellular interterritorial spaces. Ultrastructural examination revealed that pericellular rings contained an intralacunar component composed of microfibrils with abundant admixture of aggregates of dense amorphous non-fibrillar material. The outer extralacunar zone was made up of a layer of condensed thin collagen fibrils with admixture of non-fibrillar dense material. NGS sequencing identified a fusion transcript involving fibronectin 1 (FN1) and fibroblast growth factor receptor 2 (FGFR2) at the RNA level. At the DNA level, no significant variant was revealed except for the presumably germline variant in the *SPTA1* gene.

Introduction

Cartilaginous tumours are the most common neoplasms affecting the bone (Dorfman and Czerniak, 1998; Qasem and DeYoung, 2014; Povýšil et al., 2017; Antonescu, 2020). Conventional soft tissue cartilage-forming tumours are predominantly benign tumours, with the local recurrence rate of 17 to 18 % (Chung and Enzinger, 1978; Cates et al., 2001; Saito et al., 2017; Makni et al., 2018; Antonescu, 2020). They usually arise from the soft tissue adjacent to tendons in the hands and feet of adults. They may exhibit a variable degree of cytological atypia, including enlarged cells, moderate pleomorphism, hyperchromasia and binucleation, making it difficult to exclude a malignancy. However, the primary soft tissue chondrosarcomas are extremely rare tumours (Makni et al., 2018), and many of the reported cases were reclassified as chondromas (Chung and Enzinger, 1978; Antonescu et al., 2020). Some soft tissue chondromas show a striking resemblance to chondroblastoma of the bone (Cates et al., 2001) or contain lipoblast-like cells (Chan et al., 1986). It is well known that these tumours may undergo secon-

Received May 31, 2022. Accepted September 22, 2022.

This study was supported by the Ministry of Health, Czech Republic (Conceptual development of research organization 64165, General University Hospital in Prague) and by Charles University (Project UNCE204065).

Corresponding author: Ctibor Povýšil, Institute of Pathology, First Faculty of Medicine, Charles University and General University Hospital in Prague, Studničkova 2, 128 00 Praha 2, Czech Republic. Phone: (+420) 224 968 660; e-mail: ctibor.povysil@lf1.cuni.cz

Abbreviations: APAS staining – amylase digestion and periodic acid Schiff staining, Bcl-2 – B-cell lymphoma 2 apoptosis regulator, CK – cytokeratin, CPPD – calcium pyrophosphate deposition, CT – computer tomography, FFPE tissue – formalin-fixed, paraffin-embedded tissue, FGFR – fibroblast growing factor receptor, FN1 – fibronectin 1, FXIIIa – factor XIIIa, transglutaminase enzyme-blood coagulation factor, GFAP – glial fibrillary acid protein, IDH – isocitrate dehydrogenase, MDM2 – mouse double minute 2, MRI – magnetic resonance imaging, NGS – next-generation sequencing, ORF – open reading frame, PCM – pericellular matrix, VUS – variant of uncertain significance.

dary changes or exhibit dystrophic calcification, endochondral ossification, focal myxoid degeneration, or calcium pyrophosphate deposition (CPPD) (Athanasou et al., 1991). In a study of Amary et al. (2019), RNA sequencing identified a gene fusion involving *FNI* and fibroblast growth factor receptor 1 (*FGFR1*) in the soft tissue of classical chondromas.

In our previous work, we presented basic histological and immunohistochemical characteristics of neoplastic chondrocytes with thick amylase digestion and periodic acid Schiff staining (APAS)-positive pericellular rings occurring in some cartilage-forming tumours of the soft tissue and bone (Povýšil and Kaňa, 2021). We showed that this type of chondrocytes usually occurs as single cells or may form small groups of chondrocytes with normal phenotype surrounded with thick perichondrocytic rings. Moreover, we identified a soft tissue chondrosarcoma entirely composed of chondrocytes surrounded with thick perichondrocytic rings. We called the chondrosarcoma “chondrosarcoma with target-like chondrocytes” (Povýšil and Kaňa, 2021). Later, we identified a second chondrosarcoma with target-like chondrocytes localized in the iliac bone.

The aim of this manuscript is to present the two cartilage-forming tumours with highly unusual cell types of target-like chondrocytes surrounded with thick perichondrocytic rings (baskets). Because of the rarity of such histological pattern in chondrogenic tumours, not yet described and analysed, we present the histological, immunohistochemical, electron microscopic and molecular findings showing the morphological and molecular details of these highly abnormal cells, and provide their comparison with the chondrocytes from the bone chondrosarcomas of conventional type and soft tissue chondromas.

Material and Methods

From the archive of the Institute of Pathology of the First Faculty of Medicine of Charles University and General University Hospital in Prague, we retrieved slides and paraffin blocks of two neoplasms with neoplastic chondrocytes with an unusually thick ring surrounding the whole cell body (“target-like chondrocytes”). The unusual cell histological appearance of the cells was confirmed by comparison to 500 chondrogenic tumours of various types. The material for the present study comprised two chondrosarcomas composed of target-like chondrocytes (characterized below as Case 1 and Case 2), five conventional skeletal chondrosarcomas, and two soft tissue chondromas lacking the target-like phenotype. The follow-up information was obtained from the clinical charts. This study was approved by the Ethics Committee of the General University Hospital in Prague.

Case 1, soft tissue chondrosarcoma composed of target-like chondrocytes

The patient was a 49-year-old male. He became aware of a growing mass on the palmar side of the middle pha-

lanx of the left index finger around year 2016. Radiography revealed a tumour shadow on the palmar side of the middle phalanx of the left index finger, with foci of internal calcification without any signs of bone destruction. Magnetic resonance imaging (MRI) revealed a $60 \times 40 \times 35$ mm mass along the flexor tendon. The mass was well demarcated without signs of malignancy. After an incisional diagnostic biopsy, complete surgical excision of the tumour was performed. Until now, no recurrence of the tumour was observed.

Case 2, bone chondrosarcoma composed of target-like chondrocytes

The patient was a 56-year-old male with osteolytic mass of $40 \times 40 \times 30$ mm destructing the right iliac bone. Foci of internal calcification were present. Both radiography and computer tomography (CT) showed an ovoid, well-defined, radiolucent lesion in the iliac bone. MRI showed a well-defined homogeneous lesion in the medullary cavity of iliac bone. The outer margin of the lesion was not clearly defined, but extension into adjacent soft tissue was not evident. Patient is 8 years free of recurrence.

Histological examination

After fixation in 10% solution of formalin and tissue dehydration, the samples were processed with paraffin and sectioned into 5-micron sections. Each section was stained with haematoxylin and eosin to evaluate the general morphology and cell organization of the tumour. Staining with Alcian blue and Safranin O/Fast green enabled evaluating the content of glycosaminoglycans (Jellinghaus et al., 2018). Masson trichrome and Sirius red were used for demonstration of collagen fibres (Jones, 2002; Wachsmuth et al., 2005; Rieppo et al., 2019) and the Gomori impregnation technique was used for demonstration of reticular fibres (Ushiki, 2002). Picrosirius red detected collagens type I to V (Povýšil et al., 2017). Periodic acid Schiff (PAS) staining in diastase-treated sections showed tissue carbohydrates (neutral mucopolysaccharides) (Jones, 2002).

Immunohistochemical examination

For the purpose of immunohistochemical studies, we used the avidin-biotin complex (ABC) technique with antibodies listed in Table 1. We used the FLEX Target Retrieval solution, high or low pH for heat-induced epitope retrieval on formalin-fixed and paraffin-embedded tissue sections prior to immunohistochemical staining in a DAKO Autostainer. One part of slides were incubated for 1 h at room temperature and routinely processed with the reaction visualized using a DAKO's EnVision Flex kit with DAB chromogen in a DakoTechMate staining machine (Glostrup, Denmark). Other slides were stained with OptiView DAB IHC Detection Kit and OptiView Amplification Kit in Ventana BenchMark (Jacksonville, FL).

Staining results were scored semi-quantitatively (0 = no staining, + = weak staining, ++ = moderate to inten-

sive staining), and the staining pattern was classified as focal / diffuse / varying in intensity. For Bcl-2 (cytoplasmic reaction) and Ki67 (nuclear reaction), the percentage of positivity was determined by counting 100 cells.

The distribution of collagen types II and VI was examined by immunohistochemical reaction. Both collagen antibodies were used at a dilution of 1 : 30 after pretreatment with proteinase K (0.04 mg/ml in 0.05 mol/l Tris-HCl, pH 7.6, 5 minutes at room temperature).

Electron microscopic examination

In our present two cases, we used formalin-fixed samples from paraffin-embedded (FFPE) tissue, because glutaraldehyde-fixed material was not available. Ultrathin sections were examined under a JEM-1400 Plus Jeol electron microscope (JEOL USA, Peabody, MA). Furthermore, samples were analysed by transmission electron microscopy, and these findings were compared with our ultrastructural findings in the group of different types of chondrogenic tumours examined previously in our laboratory (Povýšil and Matějovský, 1985; Povýšil, 1986; Povýšil et al., 2017).

Next-generation sequencing

For molecular characterization of the Case 1 with target-like chondrocytes, we performed next-generation sequencing (NGS) at the RNA and DNA levels. DNA and total RNA were isolated from 10 sections (5 µm) of FFPE tissue samples by a Zymoresearch FFPE DNA/RNA isolation kit according to the manufacturer's instructions. Isolated sections contained approx. 60 % of lesional cells. After isolation, a total RNA library was processed by an ArcherDX FusionPlex Sarcoma v2 kit according to the manufacturer's protocol. A DNA sequencing library was prepared by the Roche SeqCap protocol using custom-designed hybridization probes (Roche; panel of 271 genes; target area 1020 kbp) as described before (Dundr et al., 2020). Prepared sample libraries were paired-end sequenced using NextSeq500/550 Mid Output Kit v.2.5 (Illumina) in a NextSeq 500 instrument (Illumina, San Diego, CA). The demultiplexed RNA sequencing data were analysed by Archer Analysis Software v.5.1.7. (ArcherDX, Boulder, CO) and the DNA sequencing data were analysed by NextGENe v.2.4.2. (SoftGenetics, LLC, State Collage, PA) as described in Dundr et al. (2020). RNA data analysis showed 119 Average Unique RNA Start Sites per Control GSP2. DNA data analysis showed a 906× average coverage of the targeted area.

Results

Histological examination

Chondrosarcomas with target-like chondrocytes

Both tumours had a lobular growth pattern and were composed of target-like cells. Mitoses were rare. Foci of small irregular calcification were present in intercellular spaces of some neoplastic areas, but no ossification was observed.

The soft tissue tumour (Case 1) had a distinct biphasic appearance. The minor chondrocyte component showed lobular proliferation of normal slightly hypercellular lobulated neoplastic cartilage with well-circumscribed margins. The small chondrocytes, occurring in clusters, showed minimal-to-moderate cytological atypia. The pericellular rings were distinct and thick, however without multilayering. The neoplastic stroma had a character of typical hyaline cartilage, somewhere with focal calcification. The features were those of proliferative chondroma. The major cell component was composed of larger oval cells with distinct thick perichondrocytic rings (Fig. 1A and 1B). The cartilage cells had definitely enlarged nuclei with distinct nucleoli. Binucleated cells were common, and occasionally multinucleated cells with hyperchromatic nuclei were also seen. Nuclear irregularity and hyperchromatism were in some cells prominent. The majority of cells of this atypical component possessed abundant cytoplasm, and a peculiar eosinophilic thick ring was seen around their periphery of pericellular spaces. The cell cytoplasm and the halo area surrounding the cells stained intensely with Alcian blue in 0.4M MgCl₂. In some tumour areas, single neoplastic cells with preserved perichondrocytic rings penetrated into the adjacent adipose and fibrous tissue (Fig. 1B). The cellular atypia and the signs of permeation into surrounding soft tissues suggested possible malignancy.

In the iliac chondrosarcoma (Case 2), thick perichondrocytic rings were also present in the majority of neoplastic cells (Fig. 1C). In some peripheral parts of the tumour, neoplastic cells permeated into intertrabecular spaces.

Conventional skeletal chondrosarcomas and soft tissue chondromas (control group)

The histological pattern of all five conventional chondrosarcomas and two soft tissue chondromas was characteristic of these types of tumours (Povýšil et al., 2017; Antonescu et al., 2020). All tumours showed a lobular arrangement. Compared with chondromas (Fig. 1D), the chondrosarcomas were cell-rich (Fig. 2A). In addition, some of the chondrosarcomas contained cells with hyperchromic plumb nuclei and binucleated or multinucleated cells. Neoplastic chondrocytes were usually placed in lacunae, which were however missing in less differentiated tumours.

Histochemical examination

Chondrosarcomas with target-like chondrocytes (Case 1)

The pericellular space consisted of the lacunar space surrounded with the perichondrocytic ring. Perichondrocytic rings had a homogenous structure or were composed of two or several concentric hyaline layers showing positivity for APAS (Fig. 2B). The most intensive APAS positivity occurred in the outer compact zone, in

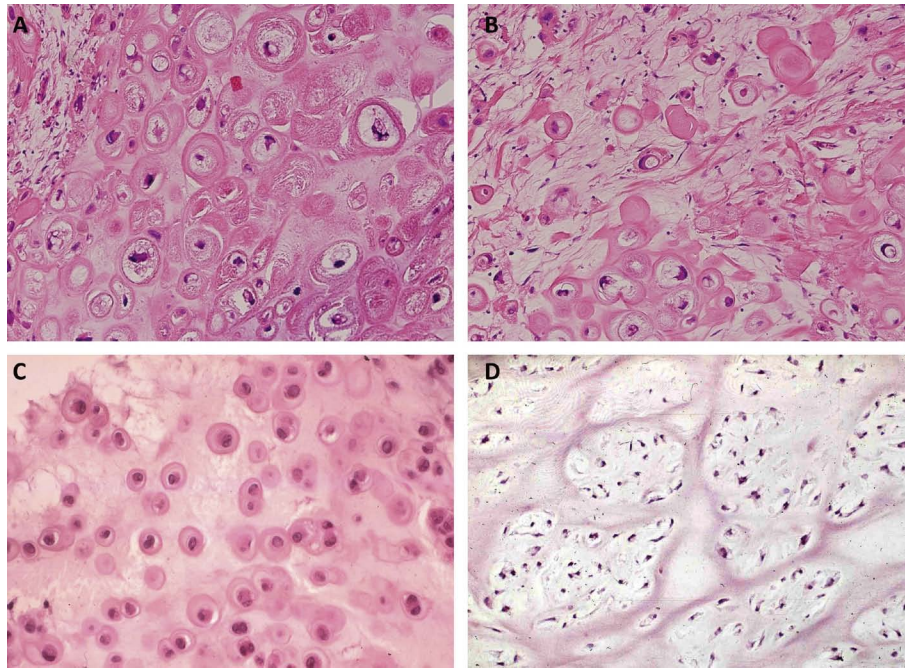


Fig. 1. (A) Case 1. Representative image of the predominating histological pattern of soft tissue chondrosarcoma with large target-like chondrocytes surrounded with eosinophilic perichondrocytic rings. Haematoxylin and eosin. Magnification 200 \times . (B) Case 1. Dissociated neoplastic chondrocytes infiltrating the surrounding fibrous tissue also had characteristic perichondrocytic rings. Moreover, some chondrons were globally sclerotic. Haematoxylin and eosin. Magnification 200 \times . (C) Case 2. Chondrosarcoma of the iliac bone was composed of small neoplastic chondrocytes with distinct perichondrocytic rings. Haematoxylin and eosin. Magnification 200 \times . (D) Representative control case of soft tissue chondroma. Haematoxylin and eosin. Magnification 140 \times .

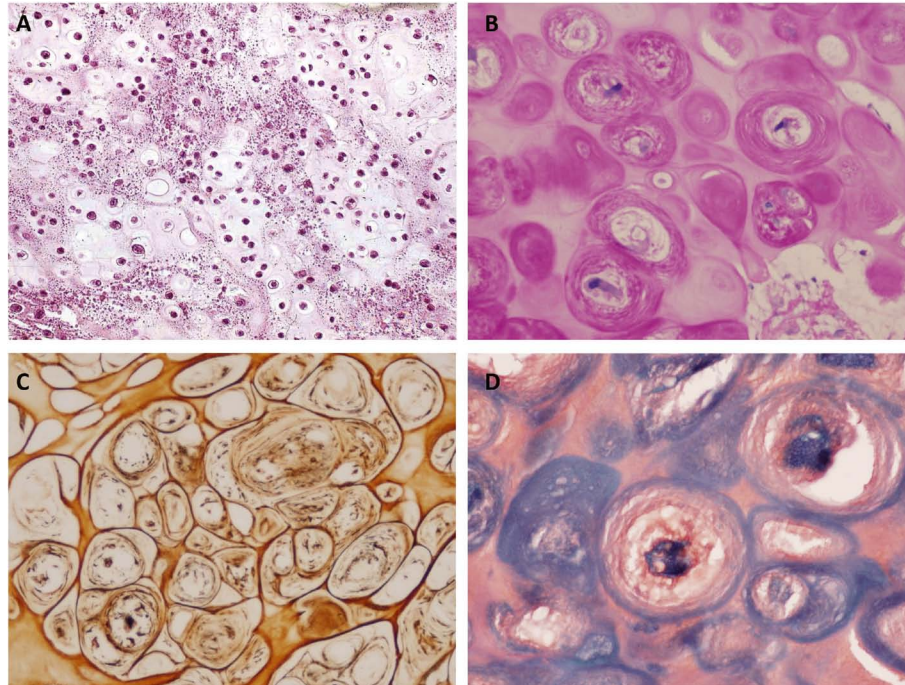


Fig. 2. (A) Control chondrosarcoma of Grade II. Histological pattern with increased cellularity and nuclear atypia. Haematoxylin and eosin. Magnification 140 \times . (B) Case 1. Detail of APAS-positive perichondrocytic rings, sometimes with signs of multilayering. APAS staining method. Magnification 400 \times . (C) Case 1. Perichondrocytic rings contain sparse silver-impregnated collagen fibres. Gomori's impregnation method. Magnification 400 \times . (D) Case 1. Safranin O/Fast green method distinguished differing composition of the material accumulated in the lacunar space (orange) from the blue perichondrocytic external part of the ring containing collagen material. Magnification 400 \times .

contrast to the inner layer that stained faintly. Moreover, in some lacunar spaces between the chondrocyte bodies and the rings, small, fragmented aggregates of APAS-positive material occurred. However, in some chondrons, these fragmented aggregates of APAS-positive material formed the majority of the perichondrocytic mass. In Masson's trichrome staining, rings had a more compact structure and stained blue as collagen. Single impregnated reticular fibres were visualized in the rings after Gomori impregnation for reticular fibres (Fig. 2C). Some lacunar spaces lacked cells and were completely substituted by APAS- and collagen-positive acellular tissue, forming together with the rings a compact round formation corresponding to globally sclerotic chondrons. Safranin O/Fast green staining revealed blue peripheral parts of perichondrocytic rings distinct from orange-stained glycosaminoglycans deposited in the lacunar perichondrocytic spaces (Fig. 2D).

Histochemical examination of the iliac bone chondrosarcoma (Case 2) corresponded to that of the soft tissue chondrosarcoma (Case 1) described above.

Conventional skeletal chondrosarcomas and soft tissue chondromas (control group)

The histochemical examination of two conventional chondromas and five chondrosarcomas did not show

APAS- or Safranin O/Fast green-positive perichondrocytic hyperplastic rings, in contrast to the target-like chondrocytes present in the chondrosarcomas in Cases 1 and 2, except for two cases in which single cells or small groups of cells had APAS-positive incomplete rings. The intercellular matrix showed staining typical of all cartilage-forming tumours.

Immunohistochemical examination

Chondrosarcoma with target-like chondrocytes (Case 1)

The results of immunohistochemical examination of the soft tissue chondrosarcoma are summarized in Table 1. The majority of the tumour cells reacted strongly, diffusely or focally, with antibodies against vimentin, factor XIIIa (FXIIIa), cyclin D1 (Fig. 3A), Bcl-2, p16, p53 and osteonectin. The S-100 protein was positive in 25 % of neoplastic cells. Antibodies against glial fibrillary acidic protein (GFAP), podoplanin (D2-40), CD99, CD10 and cytokeratin AE1.3 (CK AE1.3) exhibited weak focal positivity. No reaction was seen for CD117 (c-Kit receptor), cytokeratin CAM 5.2, EMA, alpha smooth muscle actin, muscle-specific actin, desmin, mouse double minute 2 (Mdm2), calponin, SOX10 and h-caldesmon. The alpha-methylacyl-CoA (AMACR) method was also negative. Staining with the antibody against the nuclear

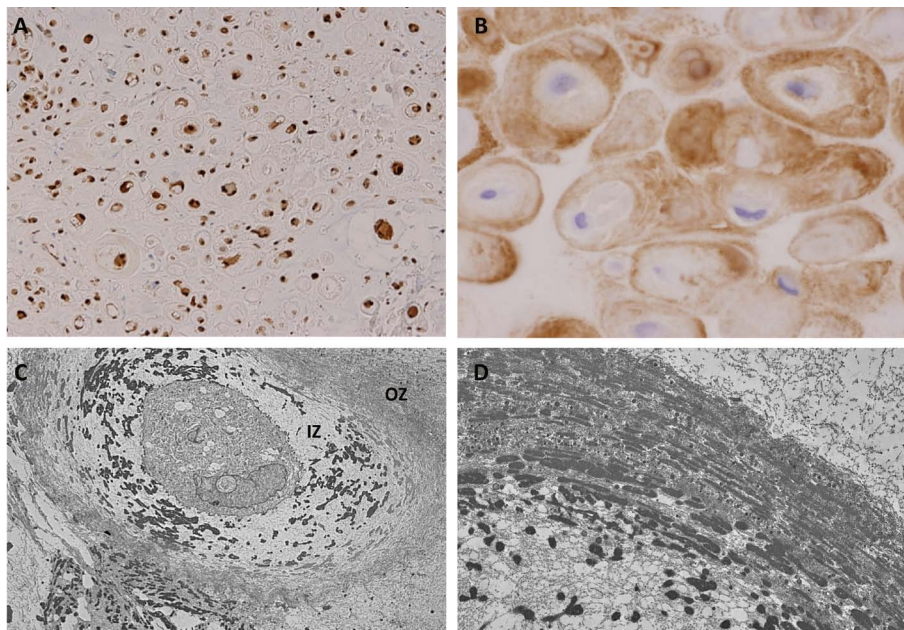


Fig. 3. (A) Case 1. Diffuse cytoplasmic and nuclear immunopositivity of cyclin D1 in soft tissue chondrosarcoma. Magnification 100 \times . (B) Case 1. Collagen VI immunopositivity in perichondrocytic rings. Magnification 400 \times . (C) Case 1. Electron microscopy of neoplastic target-like chondrocyte in lacunar space surrounded with a pericellular ring composed of two zones: the lacunar internal zone contains irregular aggregates of dense non-fibrillar material with proteoglycan granules; the outer zone is formed of a layer of condensed thin collagen fibrils with the lamellar dense material producing a capsule-like demarcation line against surrounding intercellular space. Original magnification 2500 \times . (D) Case 1. High-power view of the outer zone of perichondrocytic ring arranged in two layers composed of different dense irregular non-fibrillar and fibrillar components. Original magnification 15000 \times .

protein recognizing cells in proliferation (MIB1) showed minimal proliferative activity of about 1 % (Ki67 labeling index) in the neoplastic chondrocytes.

Immunoreactivity of type VI collagen in pericellular rings (Fig. 3B) and type II collagen in the extracellular interterritorial matrix was recognized. The antibody against type VI collagen intensively stained the peripheral parts of chondrocyte rings, small aggregates in interterritorial regions, and globally sclerotic acellular chondrons.

A limited number of immunohistochemical markers could be examined in the tissue from iliac bone chondrosarcoma in Case 2 due to the scarcity of material. The markers that could be examined showed similar reactivity to those in the soft tissue chondrosarcoma (Case 1) described above.

Conventional chondrosarcomas (control group)

Neoplastic cells showed diffuse positivity in the reaction with antibodies against S-100 protein similar to that

in target-like chondrocytes from Cases 1 and 2. There was focal positivity for p16, GFAP, CD10, CD99, Bcl-2 and podoplanin. We did not observe positive reactions with antibodies against p53, cyclin D1, FXIIIa and osteonectin in the cells from the control group (Table 1). The expression of FXIIIa and osteonectin in target-like chondrocytes is thus an interesting finding representing the main difference against conventional chondrosarcoma and benign chondroma.

Electron microscopy

Chondrosarcoma with target-like chondrocytes (Case 1)

Electron micrographs revealed many relatively normal appearing chondrocytes in which the intracytoplasmic rough endoplasmic reticulum, mitochondria, glycogen granules and lipid droplets were prominent. Chondrocytes of different shapes were deposited in round lacunar spaces containing small amounts of proteoglycan

Table 1. List of antibodies

Name	Clone	Supplier	Dilution	ChTLC	CCh
Vimentin	V9	Dako	1 : 100	Diffuse++	Diffuse++
S-100 protein	polyclonal	Dako	1 : 1600	Focal+	Diffuse++
FXIIIa	EP3372	Zytomed	1 : 200	Diffuse++	0
Osteonectin	15G12	Novocastra	1 : 40	Diffuse++	0
Bcl-2 oncoprotein	124	Dako	1 : 100	Diffuse+	Focal+
Cyclin D1	EP12	Dako	RTU	Diffuse++	0
P16	JC2	DBS	1 : 200	Diffuse++	Focal +
P53	BP-53-12	Zytomed	1 : 200	Focal+	0
GFAP	GF2	Dako	1 : 1000	Focal+	Focal+
CD10	5666	Novocastra	1 : 100	Focal+	Focal +
CD99(MIC2)	EPR 3097Y	DCS	1 : 200	Focal+	Focal+
Cytokeratin AE.3	AE1/AE3	Dako	1 : 200	Focal+	0
D2-40 (podoplanin)	D2-40	Dako	1 : 200	Focal+	Focal+
CD34 class II	QBEND10	Dako	1 : 100	Focal+	0
Alpha smooth muscle actin	1A4	Dako	1 : 800	0	0
Muscle-specific actin	HHF35	Dako	1 : 800	0	0
Desmin	D33	Dako	1 : 200	0	0
CD117, c-kit	polyclonal	Dako	1 : 200	0	0
Cytokeratin CAM 5.2		Becton Dickinson	1 : 10	0	0
EMA	E29	Dako	1 : 200	0	0
Calponin	CALP	Dako	1 : 400	0	0
SOX10	EP268	Cell Marque	1 : 400	0	0
Mdm2	SMP14	Sigma Aldrich	1 : 1000	0	0
CDX2	EPR 27G4Y	Zytomed	1 : 200	0	0
Ki67 antigen MIB1	MIB1	Dako	1 : 100	Positive 1 %	Positive 1 %

ChTLC – chondrosarcoma with target-like chondrocytes, CCh – conventional chondrosarcoma, RTU – ready-to-use.

Staining results were scored semi-quantitatively (0 – no staining, + – weak staining, ++ – moderate to +++ intense staining), and the staining pattern was noted (focal/diffuse). For Bcl-2 (cytoplasmic reaction) and Ki67 (nuclear reaction), the percentage was estimated by counting 100 cells.

granules and irregular aggregates of amorphous dense material of different sizes and shapes (Fig. 3C and 3D). Analysis of the histochemical and electron microscopic findings showed that this material corresponds to the APAS-positive aggregates deposited in the extracellular space of the lacunae – so-called inner zone (IZ). The outer zone (OZ) of the pericellular ring was formed by a layer of condensed thin collagen fibrils with admixture of less dense trabecular material oriented parallel to the chondrocyte cell bodies. It produced a capsule-like demarcation line against surrounding intercellular spaces (Fig. 3C and 3D). In some chondrons, almost the entire rings were composed of these dense aggregates with a small amount of microfibrils (Fig. 4A). The matrix of intercellular spaces contained identical thin collagen fibrils with irregular orientation organized in the form of a network (Fig. 4B). Small dense granules corresponding to glycosaminoglycans were situated in the space between microfibrils.

No material was available for electron microscopy in Case 2.

Conventional chondrosarcomas and enchondromas (control group)

The ultrastructural study of benign and malignant chondrogenic tumours revealed gradual transition from well-differentiated cells of chondromas to poorly differentiated cells resembling immature mesenchymal cells in chondrosarcomas (Fig. 4C and 4D). Distinct pericel-

lular lacunar spaces containing proteoglycan granules and small dense deposits were usually surrounded at the periphery with a narrow layer of thin collagen fibres. Numerous neoplastic cells had no distinct lacunar space and were in direct contact with the intercellular substance (Fig. 4D). The cytoplasm of the neoplastic chondrocytes contained mitochondria, Golgi apparatus, scanty lipid droplets, rather large aggregates of glycogen particles, and rough endoplasmic reticulum. Its irregular, sometimes strongly dilated cisternae contained amorphous material of intermediate density.

Molecular DNA and RNA analysis

RNA NGS sequencing of chondrosarcoma with target-like chondrocytes (Case 1)

RNA sequencing showed a highly expressed fusion transcript consisting of the *FNI* part (NM_002026.2; presumably from exon 1 to part of exon 22; chr2:216262413) and the *FGFR2* part (NM_001144916.1; chr10:123317560; internal, 82 bp part of intron 4 followed by exon 5 to final exon 15). The fusion was detected with a high coverage of 1140 reads in the fusion area, which also reflects the increased relative expression of the *FGFR2* part (6–9×) in comparison to the internal reference genes of the kit (*CHMP2A*, *GPI* and *RAB7A*). The detected fusion transcript maintains the open reading frame (ORF) for *FNI* and *FGFR2*. The fusion transcript does not contain a premature STOP co-

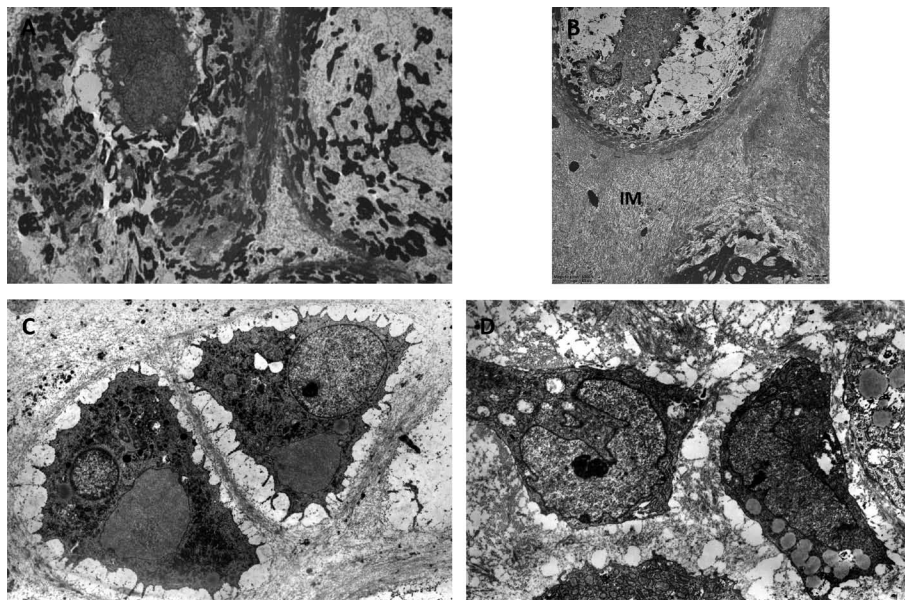


Fig. 4. (A) Case 1. Dark neoplastic chondrocyte surrounded with a ring composed only of irregular aggregates of dense non-fibrillar material. Original magnification 4000×. (B) Case 1. Detail of intercellular matrix between two chondrocytes composed of thin collagen fibrils and proteoglycan granules. Original magnification 5000×. (C) Control enchondroma. Two control neoplastic chondrocytes surrounded with thin rings composed predominantly of microfibrillar material. Original magnification 3000×. (D) Control malignant chondrocyte from Grade II chondrosarcoma without ring is surrounded by intercellular matrix. Original magnification 3000×.

don for a particular ORF. Therefore, the fusion transcript will be translated to the FN1-FGFR2 fusion protein with high probability.

DNA NGS sequencing of chondrosarcoma with target-like chondrocytes (Case 1)

The copy number analysis of NGS DNA data revealed extensive one allele deletion of the gene targets located on chromosome 6, namely *IRF4*, *HISTH3B*, *MDC1*, *DAXX*, *FANCE*, *CDKN1A*, *RNF8*, *CCND3*, *VEGFA*, *SLC29A1*, *NT5E*, *EPHA7*, *WISP3*, *HDAC2*, *ROS1*, *ZBTB2*, *ESR1*, *ARID1B* and *QKI*. Because the targets are located across both arms of chromosome 6, we assume that one allele of the whole chromosome 6 is deleted. Further, the same analysis revealed one allele duplication of the gene targets located on chromosome 19, namely *KEAP1*, *SMARCA4*, *NOTCH3*, *BRD4*, *JAK3* and *PIK3R2*. These targets are located between p.13.2 and p.13.11 areas of chromosome 19.

Mutation analysis of the oncology-focused gene panel did not reveal any pathogenic or probably pathogenic variant except for *SPTA1* [NM_003126.2:c.6421C>T, p.(Arg2141Trp); coverage 646×; variant frequency 53 %], which is 1× rated as likely pathogenic and 3× as a variant of uncertain significance (VUS) in the ClinVar database. We further identified missense variants with uncertain significance (VUS) in *ARID1A* [NM_006015.4:c.2718C>G, p.(Asn906Lys)], *F11R* [NM_016946.4:c.301C>T, p.(Arg101Trp)], *PIK3CG* [NM_002649.2:c.1076G>A, p.(Arg359His)], *FANCF* [NM_022725.3:c.385C>G, p.(Leu129Val)], *RAD51API* [NM_001130862.1:c.487G>A, p.(Val163Ile)] and *ERG* [NM_001243432.1:c.388C>G, p.(Arg130Gly)]. All these VUS had frequencies around 50 % and are potentially germline.

Molecular analysis of skeletal conventional chondrosarcomas (control group)

According to the MSK-IMPACT study (Cheng et al., 2015), the most frequently mutated genes in conventional skeletal chondrosarcomas are isocitrate dehydrogenase 1 (*IDH1*; 26.3 % of cases) and *TP53* (10.5 % of cases). We did not detect any class 3–5 variant (unknown significance, likely pathogenic or pathogenic) in these genes in Case 1.

Discussion

Cartilage-forming tumours are a heterogeneous group of tumours with characteristic histological features (Dahlin and Salvator, 1974; Chung and Enzinger, 1978; Chan et al., 1986; Athanasou et al., 1991; Dorfman and Cierniak, 1998; Cates et al., 2001; Qasem and DeYoung, 2014; Povýšil et al., 2017; Saito et al., 2017; Makni et al., 2018; Antonescu et al., 2020). The hallmark of all differentiated chondrogenic tumours is the presence of neoplastic chondrocyte cells producing characteristic

cartilaginous tumour matrix. The tumour cells resemble normal chondrocytes of hyaline cartilage. The cells are sometimes located in lacunar spaces, some of which are surrounded with very thin rings embedded in the hyaline cartilage matrix. The intercellular substance contains glycosaminoglycans and the fibrillar component represented by collagen fibres of different types.

Extraskelatal chondroma was described by Chung and Enzinger (1978). The chondromas are predominantly located in fingers, hands, toes and feet. Less common locations include the forearms, legs, chest and visceral organs (Dahlin and Salvador, 1974; Chung and Enzinger, 1978; Cardia 2019; Antonescu et al., 2020). The cases of extraskelatal chondroma are estimated to account for about 1.5 % of all benign soft tissue tumours. Even benign chondroma may have nuclear atypia and multinuclear cells. Therefore, histopathological differential diagnosis from low-grade chondrosarcoma can be sometimes difficult. Our soft tissue tumour (Case 1) was diagnosed as a semi-malignant cartilaginous tumour based on the findings of increased cell density, scarce binuclear cells and/or multinuclear cells. However, the findings of permeation of neoplastic cells into the soft tissue in the neighbourhood suggested probable malignant potency of this neoplasm. In spite of this finding, after seven years of follow-up, no metastases were recognized. The skeletal chondrosarcoma (Case 2) had the usual histological structure, and pericellular rings were thinner in contrast to the first case, but they were still distinct in the majority of cells. No recurrence or metastasis were observed during eight years after surgical resection.

In this study, we analysed in detail an extraskelatal cartilage-forming tumour with highly specific histological features and the *FN1-FGFR2* gene fusion. The *FN1-FGFR2* fusion was previously described in four cases of a chondroblastoma-like variant of soft tissue chondroma (Amary et al., 2019; Kao et al., 2020). However, no thick perichondrocytic rings were observed in these cases. Our RNA sequencing showed a fusion between the exon 22 of *FN1* and intron 4-exon 5 of *FGFR2*, which is similar to the *FN1-FGFR2* fusion identified in the four cases of Amary et al. (2019). There was a fusion between the exon 19 of *FN1* and exon 7 of *FGFR2* in their cases. However, fusions of *FN1* to other receptor tyrosine kinases have also been detected in some other neoplasms of soft tissue tumours, including the *FN1-FGFR1* fusion in some chondromas (Amary et al., 2019), *FN1-EGF* fusion in calcifying aponeurotic fibroma (Puls et al., 2016), *FN1-FGFR1* and *FN1-FGFI* fusions in phosphaturic mesenchymal tumour (Lee et al., 2016), *FN1-AVCR2A* fusion in synovial chondromatosis (Amary et al., 2019), *FN1-ROS1* fusion in inflammatory myofibroblastic tumour (Kao et al., 2020), *FN1-ALK* fusion in gastrointestinal leiomyoma and inflammatory myofibroblastic tumour (Panagopoulos et al., 2016), and *FN1-FGFR1* fusion in ALK-negative inflammatory myofibroblastic tumour (Kao et al., 2020).

Our DNA sequencing suggested heterozygous deletion of the whole chromosome 6 and duplication of part

of chromosome 19, as detected by the copy number variation analysis. Moreover, mutation analysis did not reveal any interesting variant except for the *SPTA1* variant. Variants in *SPTA1* are usually associated with red blood cell diseases, and since the mutation allele frequency of the detected *SPTA1* variant is around 50 %, this may indicate that the variant could be germline, and therefore we do not associate it with the observed lesions. Interestingly, we did not identify any class 3–5 variant in the *IDH1* and *IDH2* genes, which are frequently detected in the chondrosarcoma. However, no such mutations have been detected in peripheral chondrosarcomas, mesenchymal chondrosarcomas, osteochondromas and soft tissue cartilage-forming tumours (Amary et al., 2019; Antonescu et al., 2020).

In our two tumours with target-like chondrocytes, the pericellular rings around all chondrocytes were arranged in two different manners. In the most common variant, chondrocytes of different shapes were situated in round lacunar extracellular spaces containing a small amount of proteoglycan granules, microfibrils and irregularly distributed aggregates of dense amorphous material. The outer extralacunar zone of pericellular rings was composed of thin collagen fibrils and a dense lamellar substance oriented parallel to chondrocytes and produced rather a dense capsule-like demarcation line against the surrounding matrix of intercellular interterritorial and periterritorial spaces. However, some chondrons had rings composed predominantly of multiple dense aggregates of non-fibrillar material deposited in the lacunar space that also occurred in the intercellular spaces. The almost identical dense material resembled the product concentrated in the dilated rough endoplasmic reticulum of chondrocytes of different cartilaginous neoplasms examined in our laboratory (Povýšil, 1986; Povýšil et al., 2017). Analysis of the histochemical and electron microscopic findings showed that this material corresponds to the APAS-positive aggregates of the inner zone of the pericellular ring. The matrix of intercellular interterritorial spaces also contained thin collagen type II fibrils with irregular orientation in the form of a network. In these spaces, small dense granules occurred corresponding to proteoglycans and some deposits of dense non-fibrillar material. Some lacunar spaces lacked cells and were completely substituted by APAS-, Masson- and Safranin O-positive acellular tissue forming, together with the rings, a compact round formation corresponding to globally sclerotic chondrons containing a large amount of type VI collagen and some reticular fibres.

Histological review of one part of our collection of chondrogenic tumours showed similar cells with thick perichondrocytic rings in some cartilage-forming neoplastic lesions (Povýšil and Kaňa, 2021). This phenomenon had a sporadic occurrence, sometimes associated with calcification or ossification in some osteochondromas and soft tissue chondromas (Povýšil and Kaňa, 2021). Old paraffin-embedded tissue was not suitable for the molecular analysis. However, incomplete rings

of the cells did not contain any blue-stained component composed of predominantly collagen fibres in the Safranin O staining method.

Only a relatively small number of studies have studied chondrosarcoma by immunohistochemistry in detail, and these reports have not defined a specific immunophenotype of conventional chondrosarcoma (Park et al., 1996; Oshiro et al., 1998; Hameetman et al., 2005; Ordonez, 2006; Daugaard et al., 2009; Liu et al., 2015; Jeong and Kim, 2018). Therefore, we have attempted to carefully discriminate the immunophenotype of neoplastic cells in our cases with hyperplastic rings from conventional bone chondrosarcoma. The positivity of S-100 protein and D2-40 (podoplanin) seems to be highly consistent with the diagnosis of chondrosarcoma. Of great significance was also the finding of rather strong immunoreactivity for vimentin, S-100 protein, factor XIIIa, Bcl-2, cyclin D1, p53, p16 and osteonectin. A generally moderate or weak reaction was seen for D2-40 (podoplanin), CD99, CD10, GFAP and cytokeratin AE1.3 (CK-AE1.3). The results of some reactions were identical with those described in the literature (Park et al., 1996; Oshiro et al., 1998; Hammetman et al., 2005; Ordonez, 2006; Daugaard et al., 2009; Liu et al., 2015; Jeong and Kim, 2018). Original findings include immunopositivity for factor XIIIa, CD99, CD10 and CK-AE 1.3 in chondrogenic tumours. However, the significance of these findings is unclear because all these markers are expressed in a variety of neoplasms of different histogenesis. Osteonectin and FXIIIa were completely negative in the control group of tumours that lacked the target-like cells. The expression of these markers in the chondrosarcoma with the *FNI-EGFR2* gene fusion (Case 1) may be associated with the recognized genetic change. However, some authors (Daugaard et al., 2009) also observed positive expression of osteonectin in some conventional osteosarcomas. The focal positivity of p16 probably has prognostic implication, because the loss of expression of this marker occurs in some malignant tumours (Daugaard et al., 2009; Liu et al., 2015). Some reports have indicated a correlation between the loss of p16 expression and high-grade central chondrosarcoma (Asp et al., 2001).

The positivity for MDM2 correlates well with aggressive behaviour, as was observed by Daugaard et al. (2009) in their study of chondrosarcomas. In our cases, the MDM2 reaction was negative. However, over-expression of the *p53* gene may indicate possible aggressive behaviour of our tumour (Oshiro et al., 1998). Our soft tissue tumour had less than 25 % of positive tumour cell nuclei. Cyclin D1, p16 and MIB1 levels might be of value in predicting the histological grade and prognosis of chondrosarcoma (Daugaard et al., 2009; Liu et al., 2015). Moreover, Jeong and Kim (2018) proposed as a new marker alpha-methylacyl-CoA racemase (AMACR) for differential diagnosis of enchondroma and chondrosarcoma. In our tumour, this marker was negative. The positivity for Bcl-2 could confirm the probable malignancy of our soft tissue tumour, as it is considered a

valuable diagnostic marker for malignant chondrogenic tumours (Hameetman et al., 2005).

Ota et al. (1995) demonstrated, in extraskeletal cartilage tumours, immunoreactivity of type VI collagen in the pericellular area and type II collagen in the extracellular matrix. The results of immunohistochemical examination in our tumours were similar. It is possible to suppose that secretion of collagen and proteoglycans in the chondrocytes with thick pericellular rings has changed during the development of the neoplasm, perhaps under the influence of some changes of local conditions and perhaps also in association with some fusion of genes. This process led to exaggerated production of both non-fibrillar and fibrillar components, and they accumulated at the site of lacunar space and perichondrocytic ring, where the material was retained. We observed accumulation of identical dense amorphous material in the matrix of some bone chondrogenic tumours by electron microscopy (Povýšil, 1986). In contrast to the present Cases 1 and 2, this product did not accumulate in pericellular lacunae, but was irregularly distributed in small amounts in the intercellular matrix of the neoplasms, and the histological pattern of the tumour was not modified (Povýšil, 1986).

Chondrons represent a distinct functional compartment within the articular cartilage. The articular non-neoplastic chondrocytes are situated in lacunar spaces surrounded with a thin ring composed of type VI collagen fibres (Söder et al., 2002). The collagen in the pericellular matrix shows a basket-like morphology (Guilak et al., 2018). This unique region is called “pericellular matrix” (PCM), which integrates with the surrounding tissue via the “periterritorial matrix” connecting the PCM to the “interterritorial matrix.” Together, the chondrocyte and its PCM have been termed the “chondron” (Poole, 1997; Guilak et al., 2018; Hallett and Ono, 2019). Chondrons are primary functional and metabolic units of cartilage protecting the integrity of chondrocytes (Guilak et al., 2018). Chondrons were found to contain a large amount of proteoglycans (Roughley and Lee, 1994; Watanabe, 2004) and collagen types II, VI, and IX (Young et al., 2000; Zelenski et al., 2015; Antonescu et al., 2020). Type VI collagen anchors the chondrocytes to PCM through beta-integrin receptors and through transmembrane proteoglycans NG2 (Matsumoto et al., 2006). Type VI collagen forms interfaces in between the cell surface and the type II collagen network. PCM also significantly influences chondrocyte genes. Cartilage matrix turnover is a slow, continuous process. As PCM surrounds every chondrocyte, all matrix components secreted by chondrocytes must pass through this region (Poole et al., 1987; Marcelino and McDevitt, 1995; Poole et al., 1997; Wilusz et al., 2014). We suppose that similar conditions to those existing in the chondrons of articular cartilage also exist in cartilage-forming tumours. On the basis of our experience and that of Poole et al. (1985), the rings of neoplastic chondrocytes usually contain only sparse thin type II collagen fibrils. Due to the avascular nature of neoplastic cartilage, the im-

mediate pericellular environment of the chondrocytes appears to play a critical role in regulating cell activity, as it is supposed in articular cartilage (Poole et al., 1985; Eyre, 2001).

Little is known about the synthetic rates of various collagen types and proteoglycans in chondrogenic tumours. However, they can be supposed to be similar to those in the hyaline articular cartilage. The hyaline articular cartilage is mainly composed of water, different types of collagens, proteoglycans and chondrocytes. The histological appearance of chondrocytes of our two cases resembled, to a certain degree, that of chondrocytes occurring in the iliac crest growing cartilage in diastrophic dysplasia (Horton et al., 1979; Stöss and Pesch, 1985; Shapiro, 1992; Mařík et al., 2015) and type 1B achondrogenesis (Corsi et al., 2001). The pericellular rings were also APAS positive, but electron microscopic study revealed a different structural composition, in contrast to pericellular rings observed in our tumours. In diastrophic dysplasia, the rings were formed by extremely broad collagen fibres resembling amiantoid fibres (Horton et al., 1979; Mařík et al., 2015). However, they differed from the amiantoid fibres occurring in the hyaline cartilage as a result of degeneration (Ghadially et al., 1979; Mallinger and Stockinger, 1988). However, no characteristic clinical and radiologic features of these genetic disorders (mutation of *SLC26A2*) were observed in our patients suffering from the described chondrogenic tumours. We also examined cartilage samples from three patients with diastrophic dysplasia (Mařík et al., 2015), and our findings were identical with literature facts (Horton et al., 1979; Stöss and Pesch, 1985; Shapiro, 1992). It is well known that metabolic needs of chondrocytes are lower than those of other tissues. In chondrosarcomas, there is a higher proliferating capillary index than in benign chondrogenic tumours (Kalinski et al., 2009). Angiogenesis is an important factor in the tumour growth and progression. In our recent study (unpublished data focused on the morphological changes of chondrocytes in auricular cartilage grafts), it was proved that auricular cartilage grafts remained compact and partially vital, but the number of surviving chondrocytes was reduced in the removed grafts after several years. We also observed empty lacunae, where lacking chondrocytes were substituted with collagen fibres. This finding shows that cartilage is able to survive in hypoxic environments and moreover, that chondrocytes can continue in their synthetic activity and produce different components of the cartilage matrix in such conditions. It is known that chondrocytes possess highly effective adaptation mechanisms (Wenger and Gassman, 1997; Distler et al., 2004). New observations indicate that hypoxia-inducible factor 1 alpha (HIF-1 α) allows chondrocytes to survive extremely low oxygen tension (Wenger and Gassman, 1997; Distler et al., 2004; Pfander and Gelse, 2007; Dennis et al., 2020). Angiogenic and hypoxic signalling also plays an important role in chondrosarcoma progression (Boeuf et al., 2010). On the other hand, some experimental results indicated that cartilage sheets

formed at physiological oxygen tension (5 %) contained greater amounts of glycosaminoglycans and type II collagen (Dennis et al., 2020) than those cultured in atmospheric oxygen (20 %). We do not exclude that oxygen tension in neoplastic cartilage could also play a role in the development of thick perichondrocytic rings observed in our cases, because some chondrons were also completely replaced by homogeneous fibrous tissue. The collagenous matrix of cartilage is a highly complex assemblage of multiple gene products. All these functions, including molecular mechanisms, are not yet well understood. Better insight into the molecular mechanisms by which chondrocytes control the functional integrity of the collagenous component of adult articular cartilage (Corsi et al., 2001) and cartilaginous neoplasms is needed.

In summary, this is the first histological and molecular analysis describing details of the composition of unusual thick APAS-positive pericellular rings observed in two cases of soft tissue and bone chondrosarcoma. Such cartilage-forming tumours with target-like cells are the first such chondrosarcomas reported in the literature according to our knowledge. There was a *FNI-FGFR2* gene fusion and allele deletion of the examined targets on chromosome 6 with allele duplication of the targets on chromosome 19. Analysis of our files showed that a cartilaginous tumour composed entirely of target-like chondrocytes is a highly uncommon histological pattern with poorly understood histogenesis and aetiopathogenesis. The clinical significance of this tumour subvariant is also unclear. However, some chondroid tumours may contain a small admixture of neoplastic cells with similar histological features characterized by the thick pericellular rings, as previously reported by Povýšil and Kaňa (2021).

Credit authorship contribution statement

Ctibor Povýšil: histology and immunohistochemical examination, conceptualization, investigation, validation, writing – original draft, supervision. Martin Kaňa: formal analysis, writing – review and editing, visualization, electron microscopy. Jan Hojný: methodology of molecular analysis, analysis, investigation, validation.

Conflict of interest

The authors declare that they have no conflict of interest.

References

- Amary, L., Peres-Casanova, H. Y. E. L., Cottone, L. A., Strobl, S., Cool, P. (2019) Synovial chondromatosis and soft tissue chondroma: extraosseous cartilaginous tumours defined by *FNI* gene rearrangement. *Mod. Pathol.* **32**, 1762-1771.
- Antonescu, C. R., Bridge, J. A., Cunha, I. W., Dei Tos, A. P., Fletcher, C. D. M., Folpe, A. L., Goldblum, J. R., Hornick, J. L., Miettinen, M., Oda, Y. (2020) WHO classification of tumours. Soft tissue and bone tumours. 1st chapter. Soft tissue tumours. In: *Soft Tissue and Bone Tumours*, 5th Ed. IARC, Lyon.
- Asp, J., Inerot, S., Block, J. A., Lindahl, A. (2001) Alterations in the regulatory pathway involving p16, PRb and cdk4 in human chondrosarcoma. *J. Orthop. Res.* **19**, 149-154.
- Athanasou, N. A., Caughey, M., Burge, P., Woods, C. G. (1991) Deposition of calcium pyrophosphate dihydrate crystals in soft tissue chondromas. *Ann. Rheum. Dis.* **50**, 950-952.
- Boeuf, S., Bovee, B., Lehner, B., Hogendorn, P. C., Richter, W. (2010) Correlation of hypoxic signaling to histological grade and outcome in cartilage tumours. *Histopathology* **56**, 641-651.
- Cardia, R., Favazzi, C., Fenga, M. D., Rosa, M. A., Leni, A. (2019) A large extraskeletal chondroma: an unusual location in the lower extremity, huge extraskeletal chondroma: an unusual localization in the leg. *J. Orthop. Case Rep.* **9**, 74-77.
- Cates, J. M., Rosenberg, A. E., O'Connell, J. X., Nielsen, G. P. (2001) Chondroblastoma-like chondroma of soft tissue: an underrecognized variant and its differential diagnosis. *Am. J. Surg. Pathol.* **25**, 661-666.
- Chan, J. K., Lee, K. C., Saw, D. (1986) Extraskeletal chondroma with lipoblast-like cells. *Hum. Pathol.* **17**, 1285-1287.
- Cheng, D. T., Mitchell, T. N., Shah, R. H., Benayed, R., Syed, A., Chandramohan, R., Liu, Z. Y., Won, H. H., Scott, S. N., Brannon, A. R., O'Reilly, C., Sadowska, J., Casanova, J., Yannes, A., Hechtman, J. E., Yao, J., Song, W., Ross, D. S., Oultache, A., Dogan, S., Borsu, L., Hameed, M., Nafa, K., Arcila, M. E., Ladanyj, M., Berger, M. F. (2015) Memorial Sloan Kettering-Integrated mutation profiling of actionable cancer targets (MSK-IMPACT): a hybridization capture-based next generation sequencing clinical assay for solid tumor molecular oncology. *J. Mol. Diagn.* **17**, 251-264.
- Chung, E. B., Enzinger, F. M. (1978) Chondroma of soft part. *Cancer* **11**, 1414-1424.
- Corsi, A., Rimunucci, M., Fischer, L. W., Bianco, P. (2001) Achondrogenesis type IB. *Arch. Pathol. Lab. Med.* **125**, 1375-1378.
- Dahlin, D. C., Salvador, A. H. (1974) Cartilaginous tumours of the soft tissues of the hands and feet. *Mayo Clin. Proc.* **49**, 721-726.
- Daugaard, S., Christensen, L. H., Hogdall, H. (2009) Markers aiding the diagnosis of chondroid tumours: an immunohistochemical study including osteonectin, bcl-2, cox-2, actin, calponin, D2-40 (podoplanin), mdm-2, CD117(c-kit), and YKL-40. *APMIS* **117**, 518-525.
- Dennis, J. E., Whitney, J., Rai, J., Fernandes, R. J., Kean, T. J., (2020) Physioxia stimulates extracellular matrix deposition and increases mechanical properties of human chondrocyte-derived tissue-engineered cartilage. *Front. Bioeng. Biotechnol.* **8**, 590743.
- Distler, J. H. W., Wenger, M., Gassman, M., Kurowska, A., Hirth, S., Gay, S., Distler, O. (2004) Physiological responses to hypoxia and implications for hypoxia-inducible factors in the pathogenesis of rheumatoid arthritis. *Arthritis Rheum.* **50**, 10-23.
- Dorfman, H. D., Czerniak, B. (1998) *Bone Tumors*, 1st Ed. Mosby, St. Louis.

- Dundr, P., Věcková, Z., Tichá, I., Hojný, J., Němejcová, K., Bártů, M. (2020) Microscopic extraovarian sex cord proliferation: report of a case with bilateral Fallopian tube involvement and comprehensive molecular analysis. *Pol. J. Pathol.* **71**, 175-180.
- Eyre, D. (2001) Articular cartilage and changes in arthritis: collagen of articular cartilage. *Arthritis Res.* **4**, 30-42.
- Ghadially, F. N. E., Lalonde, J. M. A., Yong, N. K. (1979) Ultrastructure of amianthoid fibers in osteoarthrotic cartilage. *Virchows Arch. B Cell Pathol. Incl. Mol. Pathol.* **31**, 81-86.
- Guilak, F., Nims, R., Dicks, A., Wu, C. L., Meulenbelt, I. (2018) Osteoarthritis as a disease of the cartilage pericellular matrix. *Matrix Biol.* **71-72**, 40-50.
- Hallett, S. A., Ono, W., Ono, N. (2019) Growth plate chondrocytes: skeletal development, growth and beyond. *Int. J. Mol. Sci.* **20**, 6009.
- Hameetman, L., Kok, P., Eilers, P. H. C., Cleton-Jansen, A. M., Hogendoorn, P. C. V., Bovek, J. V. M. G. (2005) The use of bcl-2 and PTHLH immunohistochemistry in the diagnosis of peripheral chondrosarcoma in a clinicopathological setting. *Virchows Arch.* **446**, 430-437.
- Horton, A., Rimoin, D. L., Hollister, D. W., Silberberg, X. (1979) Diastrophic dwarfism: a histochemical and ultrastructural study of the endochondral growth plate. *Pediatr. Res.* **13**, 904-909.
- Jellinghaus, K., Hachman, C., Höland, K., Bohnert, M., Wittwer-Backofen, U. (2018) Collagen degradation as a possibility to determine the post-mortem interval (PMI) of animal bones: a validation study referring to an original study. *Int. J. Legal Med.* **132**, 753-763.
- Jeong, W., Kim, H. J. (2018) Biomarkers of chondrosarcoma. *J. Clin. Pathol.* **71**, 579-583.
- Jones, M. L. (2002) Connective tissue and stains. In: *Theory and Practice of Histological Techniques*, eds. Bancroft, J. D., Gamble, M., pp. 139-162, 5th edition. Churchill Livingstone, London.
- Kalinski, T., Sel, S., Kouznetsova, I., Rörke, M., Roessner, A. (2009) Heterogeneity of angiogenesis and blood vessel maturation in cartilage tumours. *Pathol. Res. Pract.* **205**, 339-345.
- Kao, Z. C., Lee, J., Huang, H. Z. (2020) What is new about the molecular genetics in matrix-producing soft tissue tumours? The contributions to pathogenetic understanding and diagnostic classification. *Virchows Arch.* **476**, 121-134.
- Lee, J. C., Su, S. Y., Changou, C. A., Yang, R. S., Tsai, K. S., Collins, M. T., Orwoll, E. S., Lin, C. Y., Shih, S. R., Lee, C. H., Oda, Y., Billings, S. D., Li, C. F., Nielsen, G. P., Konishi, E., Petersson F., Carpenter, T. O., Sittampalan, K., Huang, H. Y., Folpe, A. L. (2016) Characterization of *FNI-FGFR1* and novel *FNI-FGF1* fusion genes in a large series of phosphaturic mesenchymal tumours. *Mod. Pathol.* **29**, 1335-1346.
- Liu, J., Zhang, Q., Wang, Z. (2015) Clinicopathological significance of p16, cyclin D1, Rb and MIB-1 levels in skull base chordoma and chondrosarcoma. *World J. Otorhinolaryngol. Head Neck Surg.* **1**, 50-56.
- Makni, S. W., Makni, S. K., Triki, F. E., Mellouli, M., Abid, N., Kallel, R., Chaufi, S., Boudawarl, T. S. (2018) Well-differentiated extraskeletal chondrosarcoma: about a new case. *Pathologica* **110**, 103-105.
- Mallinger, R., Stockinger, L. (1988) Amianthoid (asbesthoid) transformation: electron microscopical studies on aging human costal cartilage. *Am. J. Anat.* **181**, 23-32.
- Mařík, I., Zemková, D., Koukolík, M., Křepelková, A., Kozłowski, M., Povýšil, C. (2015) Diastrophic dysplasia: a review and a case study. *Pohybové ústrojí* **22**, 293-326. (in Czech)
- Marcelino, J., McDevitt, C. A. (1995) Attachment of articular chondrocytes to the tissue form of type VI collagen. *Biochim. Biophys. Acta* **1249**, 180-188.
- Mallinger, R., Stockinger, L. (1988) Amianthoid (asbesthoid) transformation: electron microscopical studies on aging human costal cartilage. *Am. J. Anat.* **181**, 23-32.
- Matsumoto, K., Kamlya, N., Suwan, K., Atsumi, F., Shimizu, K., Shinomura, T., Yamada, Y., Kimata, K., Watanabe, H. (2006) Identification and characterization of versican/PD-M aggregates in cartilage. *J. Biol. Chem.* **281**, 8257-8263.
- Ordóñez, N. G. (2006) Podoplanin: a novel diagnostic immunohistochemical marker. *Adv. Anat. Pathol.* **13**, 83-88.
- Oshiro, Y., Chaturvedi, V., Hayden, D., Nazeer, T., Johnson, M., Johnston, D., Ordóñez, N. G., Ayala, A. G., Czerniak, B. (1998) Altered p53 is associated with aggressive behavior of chondrosarcoma: a long term follow-up study. *Cancer* **83**, 2324-2334.
- Ota, M., Oda, Y., Nakanishi, I. (1995) Immunohistochemical study on collagenous proteins and biophysical analysis of crystals in extraskeletal chondroma. *Pathol. Int.* **45**, 598-601.
- Panagopoulus, I., Gorunova, L., Lund-Iversen, M., Lobmaier, I., Bjerkehagen, B., Heim, S. (2016) Recurrent fusion of the genes *FN1* and *ALK* in gastrointestinal leiomyomas. *Mod. Pathol.* **29**, 1415-1423.
- Park, Y. K., Yang, M. H., Park, H. R. (1996) The impact of osteonectin for differential diagnosis of osteogenic bone tumours: an immunohistochemical and in situ hybridization approach. *Skeletal Radiol.* **25**, 13-17.
- Pfänder, D., Gelse, K. (2007) Hypoxia and osteoarthritis: how chondrocytes survive hypoxic environments. *Curr. Opin. Rheumatol.* **19**, 457-462.
- Poole, C. A. (1997) Articular cartilage chondrons: form, function and failure. *J. Anat.* **191**, 1-13.
- Poole, C. A., Flint, M. H., Beaumont, B. W. (1987) Chondrons in cartilage. Ultrastructural analysis of the pericellular microenvironment in adult human articular cartilage. *J. Orthoped. Res.* **5**, 509-522.
- Povýšil, C. (1986) Histopathology and ultrastructure of tumours and tumour-like lesions of bone. *Acta Univ. Carol. Med. Monogr.* **116**, 1-204.
- Povýšil, C., Kaňa, M. (2021) Target-like chondrocytes with thick perichondrocytic rings in cartilage forming tumours. Preliminary report. *Biomed. Pap. Med. Fac. Univ. Palacky Olomouc Czech Repub.* **165**, p. 203-208.
- Povýšil, C., Matějovský, Z. (1985) A comparative ultrastructural study of chondrosarcoma, chordoid sarcoma, chordoma and chordoma periphericum. *Path. Res. Pract.* **179**, 546-559.

- Povýšil, C., Mařík, I., Maříková, A., Horák, M. (2017) *Pathomorphology of Bone and Articular Diseases*. Galén, Prague. (in Czech)
- Puls, F., Hofvander, J., Magnusson, J., Nilsson, J., Haywood, E., Sumathi, V. P., Mangham, D. C., Kindblom, L. G., Mertens, F. (2016) FN1-EGFR gene fusions are recurrent in calcifying aponeurotic fibroma. *J. Pathol.* **238**, 502-507.
- Qasem, S. A., DeYoung, B. R. (2014) Cartilage-forming tumours. *Semin. Diagn. Pathol.* **30**, 10-20.
- Rieppo, L., Janssen, L., Rahunen, K., Lehenkari, P., Finnila, M. A. J., Saarakkala, S. (2019) Histochemical quantification of collagen content in articular cartilage. *PLoS One* **14**, e0224839.
- Roughley, P. J., Lee, E. R. (1994) Cartilage proteoglycans: structure and potential functions. *Microsc. Res. Tech.* **28**, 385-397.
- Saito, S., Nishimoto, K., Nakayama, R., Kikuta, K., Nakamura, M., Matsumoto, M., Morioka, H. (2017) Extraskel-etal chondroma of the index finger. A case report. *Case Rep. Oncol.* **10**, 479-484.
- Shapiro, F. (1992) Light and electron microscopic abnormalities in diastrophic dysplasia growth cartilage. *Calcif. Tissue Int.* **51**, 324-331.
- Stöss, J. H., Pesch, H. J. (1985) Structural changes of collagen fibrils in skeletal dysplasias. Ultrastructural findings in the iliac crest. *Virchows Arch. A Pathol. Anat. Histopathol.* **405**, 341-364.
- Söder, S., Hambach, L., Lissner, R., Kirchner, T., Aigner, T. (2002) Ultrastructural localization of type VI collagen in normal adult and osteoarthritic human articular cartilage. *Osteoarthritis Cartilage* **10**, 464-470.
- Ushiki, T. (2002) Collagen fibers, reticular fibers and elastic fibers. A comprehensive understanding from a morphological viewpoint. *Arch. Histol. Cytol.* **65**, 109-126.
- Wachsmuth, L., Söder, S., Fan, Z., Finger, Z., Aigner, T. (2005) Immunolocalization of matrix proteins in different cartilage subtypes. *Histol. Histopathol.* **21**, 477-485.
- Watanabe, H. (2004) Cartilage proteoglycan aggregate: structure and function. *Clin. Calcium* **14**, 9-13.
- Wenger, R. H., Gassman, M. (1997) Oxygen(es) and the hypoxia-inducible factor 1. *Biol. Chem.* **378**, 609-616.
- Wilusz, R. E., Sanchez-Adams, J., Guilak, F. (2014) The structure and function of the pericellular matrix of articular cartilage. *Matrix Biol.* **39**, 25-32.
- Young, R. D., Laurence, P. A., Duance V. C., Aigner, Monaghan P. (2000) Immunolocalization of collagen types II and III in single fibrils of human articular cartilage. *J. Histochem. Cytochem.* **48**, 423-432.
- Zelenski, N. A., Leddy, H. A., Sanchez-Adams, J., Zhang, J., Bonaldo, P., Liedtke W. (2015) Collagen VI regulates pericellular matrix properties, chondrocyte swelling and mechanotransduction in articular cartilage. *Arthritis Rheumatol.* **67**, 1286-1294.